

# Correlation of the phonon characteristics and microwave dielectric properties of the $\text{Ba}(\text{Mg}_{1/3}\text{Ta}_{2/3})\text{O}_3$ materials

Hsiu-Fung Cheng<sup>a,\*</sup>, Chia-Ta Chia<sup>a</sup>, Hsiang-Lin Liu<sup>a</sup>,  
Mei-Yu Chen<sup>a</sup>, Yuan-Tai Tzeng<sup>a</sup>, I-Nan Lin<sup>b</sup>

<sup>a</sup> Department of Physics, National Taiwan Normal University, Taipei 116, Taiwan, ROC

<sup>b</sup> Department of Physics, Tamkang University, Taipei 251, Taiwan, ROC

Available online 20 February 2007

## Abstract

The  $\text{Ba}(\text{Mg}_{1/3}\text{Ta}_{2/3})\text{O}_3$ , BMT, materials possess the highest quality factor ( $Q \times f$ ) in microwave frequency regime among the microwave dielectric materials and can potentially be used for high frequency communication application. To understand the mechanism that determines microwave dielectric properties of the BMT materials, spectroscopic techniques including Raman and Fourier transform infrared (FTIR) analyses are used for investigating the phonon characteristics of the materials. The Raman-shift ( $\Delta\omega_j$ ) of the Raman peaks and the resonance frequency ( $\omega_{0j}$ ) of the FTIR peaks vary insignificantly among the samples, which correlate very well with the phenomenon that the  $K$ -values for these materials are similar with one another. In contrast, the full-width-at-half-maximum (FWHM) of the Raman peaks and the damping coefficient ( $\gamma_j$ ) of the FTIR peaks vary markedly among the samples. The high- $Q$  materials possess sharpest vibrational modes, viz., smallest FWHM value for Raman peaks and smallest  $\gamma_j$  value for FTIR peaks and vice versa. The intimate relationship between the phonon characteristics and the fine structure of the materials is confirmed.

© 2006 Elsevier Ltd. All rights reserved.

**Keyword:** Dielectric properties; Raman; FTIR spectroscopies

## 1. Introduction

Complex perovskite compounds with the chemical formula  $\text{Ba}(\text{B}'_{1/3}\text{B}''_{2/3})\text{O}_3$ , where  $\text{B}'$  is Zn, Mg, Ni, or Mn and  $\text{B}''$  is Nb or Ta, exhibit ultra-low dielectric losses at microwave frequencies<sup>1</sup> when the materials possess  $\text{B}'\text{--B}''$  1:2 ordered arrangement with a structural symmetry described by the  $P\bar{3}m1$  ( $D_{3d}^3$ ) space group.<sup>2</sup>

Since the dielectric properties in microwave range follow mainly from ionic polarization, the phonon vibration spectra of  $\text{Ba}(\text{B}'_{1/3}\text{B}''_{2/3})\text{O}_3$  have been of particular interest. Tamura et al.<sup>3</sup> first analyzed the vibration of 1:2 ordered  $\text{Ba}(\text{Zn}_{1/3}\text{Ta}_{2/3})\text{O}_3$  normal modes, and Siny et al.<sup>4</sup> investigated the Raman spectra of several complex perovskites, proposing the existence of short-range 1:1 order in  $\text{Ba}(\text{Mg}_{1/3}\text{Ta}_{2/3})\text{O}_3$ . Recently, Chia et al.<sup>5</sup> and Chen et al.<sup>6</sup> studied the Raman and FTIR phonons in  $\text{Ba}(\text{Mg}_{1/3}\text{Ta}_{2/3})\text{O}_3$ , concluding that ionic sizes and the quality of 1:2 ordered structure are two important parameters that impact

the vibrational characteristics of the materials. They thus determined the dielectric properties in the microwave region based on the observation of simple perovskite  $Pm\bar{3}m$  structures.

This study investigates the Raman and FTIR spectra of  $\text{Ba}(\text{Mg}_{1/3}\text{Ta}_{2/3})\text{O}_3$ , and their relationship with microwave properties. Phonon properties are analyzed and correlated with microwave dielectric properties.

## 2. Experimental procedure

BMT ceramic samples were prepared by a conventional mixed oxide process. These samples were sintered at 1600 °C for 2–200 h in air and were then cooled at different rates (Table 1). The microwave dielectric properties were measured by the TE011 resonant cavity method using an HP 8722 network analyzer, near 6 GHz. Far-infrared and midinfrared reflectance spectra were obtained at room temperature using a Bruker IFS 66v FTIR spectrometer. The modulated light beam from the spectrometer was focused onto either the sample or an Au reference mirror, and the reflected beam was directed onto a 4.2 K bolometer detector  $\sim 40\text{--}600\text{ cm}^{-1}$  and a B-doped Si photoconductor  $\sim 450\text{--}4000\text{ cm}^{-1}$ . The different sources, beam splitters,

\* Corresponding author. Tel.: +886 2 29331075; fax: +886 2 29326408.  
E-mail address: [hfcheng@phy03.phy.ntnu.edu.tw](mailto:hfcheng@phy03.phy.ntnu.edu.tw) (H.-F. Cheng).

Table 1  
The processing conditions for preparing the Ba(Mg<sub>1/3</sub>Ta<sub>2/3</sub>)O<sub>3</sub> materials, the corresponding microwave dielectric properties and the related characteristics of the A<sub>1g</sub>(O) Raman mode

	Processing at 1600 °C		Microwave properties		A <sub>1g</sub> (O) mode	
	Sintering time (h)	Cooling rate (°C/h)	<i>K</i>	<i>Q</i> × <i>f</i> (GHz)	Raman-shift (cm <sup>−1</sup> )	FWHM (cm <sup>−1</sup> )
A	200	2	22.2	248,000	797.00	14.55
B	20	20	22.3	205,700	797.15	14.62
C	2	200	25.5	182,600	797.20	15.16

and detectors used in these studies provided substantial spectral overlap, and the reflectance mismatch between adjacent spectral ranges was less than 1%. The optical properties were calculated from a Kramers–Kronig analysis of the reflectance data.<sup>7</sup> These transformations were performed by extrapolating the reflectance at both low and high frequencies. The low-frequency extensions were determined by using the Lorentz model. In the meantime, Raman measurements were taken at room temperature, and the signals were recorded by a DILOR XY-800 triple-grating Raman spectrometer, equipped with a liquid-nitrogen-cooled CCD. The 10 mW output of the 514.5 nm line of an Ar ion laser was used as the excitation source. The obtained Raman spectra exhibited a resolution approximately 0.5 cm<sup>−1</sup>.

3. Results and discussion

The effect of the processing parameters on the microwave dielectric properties of the BMT materials is summarized in Table 1, indicating that the longer soaking time, in conjunction with slower cooling rate, leads to materials with higher *Q* × *f*-value, whereas the processing parameters seem to result in insignificant effect on the *K*-value of the samples. The crystal structures of these materials were examined using X-ray diffraction (XRD) technique to confirm that all the three samples are pure perovskite materials with *P3m1* structure. Detailed analysis using Rietvelt analysis on these XRD patterns indicates that the samples possessing larger ordering parameters show larger *Q* × *f*-values, as shown in Fig. 1 (curves a). Moreover, the dielectric constants (*K*) of the samples are intimately related to the cell volume, although the change in *K*-values among the samples is very modest. The larger cell volume (or larger lattice parameter) leads to larger *K*-value (Fig. 1, curves b), sample C.

While it is clear that the increase in ordering parameters is the main factor improving the *Q* × *f*-values of the materials,

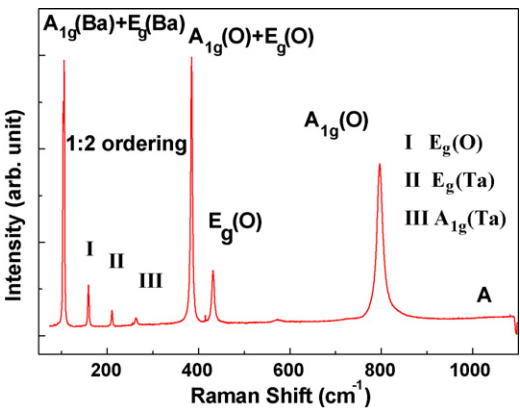


Fig. 2. Typical Raman spectra of the Ba(Mg<sub>1/3</sub>Ta<sub>2/3</sub>)O<sub>3</sub> materials.

what is the genuine mechanism for such a correlation needs more detailed studies. The Raman and FTIR spectroscopies of these materials are thus investigated. Typical Raman spectra of these BMT materials are shown in Fig. 2, indicating that the Raman peaks are very sharp, a characteristic for the high *Q* materials. Among the major Raman peaks, the A<sub>1g</sub>(O) mode at 796 cm<sup>−1</sup> varies more markedly among the samples. The characteristics of this Raman resonance peak are closely related with the microwave dielectric properties of the materials. As shown in Table 1, the shift of Raman peak is largest for the samples with largest dielectric constant (*K*<sub>C</sub> = 25.5, sample C) and is smallest for those with smallest *K*-value (*K*<sub>A</sub> = 22.2, sample A). However, the change is very modest.

In contrast, Table 1 illustrates that the width of the Raman peak (full-width-at-half-maximum, FWHM) is narrowest ((FWHM)<sub>A</sub> = 14.55 cm<sup>−1</sup>) for sample A, which possesses highest quality factor ((*Q* × *f*)<sub>A</sub> = 248,000), and is broadest ((FWHM)<sub>C</sub> = 15.16 cm<sup>−1</sup>) for sample C, which has lowest

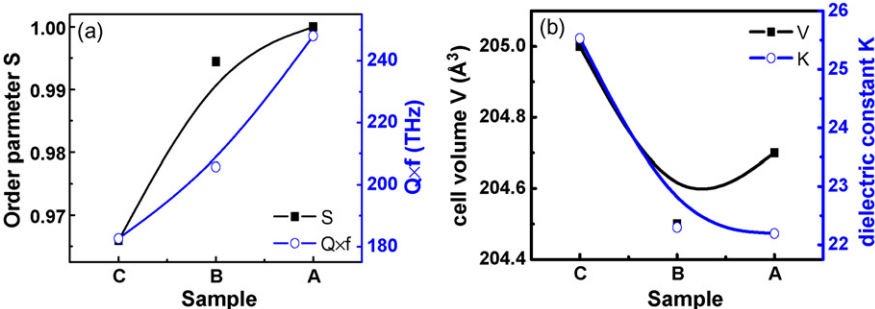


Fig. 1. The (a) ordering parameter vs. quality factor and (b) cell volume vs. dielectric constant of three Ba(Mg<sub>1/3</sub>Ta<sub>2/3</sub>)O<sub>3</sub> materials.

$Q \times f$ -value ( $(Q \times f)_C = 182,600$ ). Such kind of phenomenon is in accordance with previous reports.<sup>5</sup> Restated, the ordering of Mg- and Ta-cations is the main factor altering characteristics of Raman peaks and changing the microwave quality factor of the materials.

While the Raman spectroscopy correlates with the microwave dielectric properties of the materials very well, it cannot explain directly the dielectric response of the materials, since the Raman resonance is not a polar mode. In contrast, the Fourier transform infrared (FTIR) spectroscopy is the response of polarization of materials with respect to the electromagnetic field (infrared). Therefore, FTIR spectroscopy relates to the dielectric properties of the materials more directly. However, the analysis of the FTIR spectra is complicated. Typical reflection spectra of the BMT samples, measured in the range of 30–6500  $\text{cm}^{-1}$ , is shown in Fig. 3(a), along with the fitted data (dotted lines). The reflection spectra were analyzed using Kramers–Kronig (K–K) relationship,<sup>6</sup> in which the Lorentz distribution of the TO modes is used for fitting the spectra, i.e.,

$$\omega\varepsilon_2 = \sum_j \left( \frac{4\pi e^2 N_j}{mV} \right) \frac{\gamma_j \omega^2}{(\omega_{0j}^2 - \omega^2)^2 + \gamma_j^2 \omega^2} \quad (1)$$

$$\varepsilon_1 = \varepsilon_\infty + \sum_j \left( \frac{4\pi e^2 N_j}{mV} \right) \frac{1}{\omega_{0j}^2} = \varepsilon_\infty + \sum_j 4\pi\rho_j \quad (2)$$

$$\frac{1}{Q} = \sum_j \tan \delta_j = \sum_i \frac{4\pi\rho_j \gamma_j \omega}{\omega_{0j}^2 \varepsilon_1} \quad (3)$$

The factor analysis indicates that among the normal modes for BMT materials of  $P3m1$  symmetry,  $4A_{1g}[\text{Ba, Ta or O}] + A_{2g} + 5E_g[\text{Ba, Ta or O}] + 2A_{1u} + 7A_{2u}[\text{Ba, Mg, Ta or O}] + 9E_u[\text{Ba, Mg, Ta or O}]$ , the  $7A_{2u} + 9E_u$  modes are IR active. Out of the 16 IR active modes predicted, 15 IR peaks are identifiable, as listed in Table 2. The last one is undetected, which could be either too weak or overlaps with other modes. Fig. 3(b) shows the typical  $\omega\varepsilon_2$ -dispersion deduced from the reflection spectra using K–K analysis. It is clear from Fig. 3(b) that the  $A_{2u}(\text{Ta})$  at  $139.1 \text{ cm}^{-1}$ ,  $E_u(\text{O}_{II})$  at  $230.5 \text{ cm}^{-1}$ ,  $A_{2u}(\text{O}_{II})$  at  $245.0 \text{ cm}^{-1}$  and  $E_u(\text{Mg})$  at  $274.3 \text{ cm}^{-1}$  are the most important modes, influencing the dielectric properties of the materials, since these FTIR normal modes are of large resonance strength ( $4\pi\rho_j$ ). Such a phenomenon is in accordance with previous studies.<sup>8</sup>

Table 2

The typical IR active modes deduced from the FTIR reflection spectrum

IR peaks	$\omega_{0j} (\text{cm}^{-1})$	$\gamma_j (\text{cm}^{-1})$	$4\pi\rho_j$	Vibration modes
$\omega_{01}$	81.1	29.9	1.58	$E_u(\text{Ta})$
$\omega_{02}$	104.0	9.8	0.68	
$\omega_{03}$	139.1	3.7	3.65	$A_{2u}(\text{Ta})$
$\omega_{04}$	150.9	12.9	0.90	$E_u(\text{Ba})$
$\omega_{05}$	230.5	20.9	9.19	$E_u(\text{O}_{II})$
$\omega_{06}$	245.0	29.2	10.57	$A_{2u}(\text{O}_{II})$
$\omega_{07}$	274.3	7.6	1.62	$E_u(\text{Mg})$
$\omega_{08}$	314.7	12.8	0.82	$A_{2u}(\text{Ba})$
$\omega_{09}$	412.5	6.1	0.015	$O'$
$\omega_{10}$	434.0	13.9	0.046	$O'$
$\omega_{11}$	462.5	20.0	0.035	$O'$
$\omega_{12}$	525.3	17.8	0.273	$E_u(\text{O}_I)$
$\omega_{13}$	538.4	25.4	0.275	$O'$
$\omega_{14}$	603.1	37.6	0.415	$A_{2u}(\text{O}_I)$
$\omega_{15}$	622.2	25.5	0.346	$O'$

The resonance frequency ( $\omega_{0j}$ ) of the vibrational mode relates to the strength of Ta–O (or Mg–O) bond, which, in turn, relates to the polarizability of the Ta–O (or Mg–O) dipole and hence correlates with the dielectric constant of the materials. Fig. 4(a) (open symbols) shows that the resonance frequency of the four major vibrational modes vary insignificantly among the three BMT materials, which is in accordance with the fact that the  $K$ -values for these samples are similar with one another. In contrast, damping coefficient ( $\gamma_j$ ) of the vibrational modes relates to the coherency of Ta-layer (or O-layer) vibration, which, in turn, relates to the dielectric loss factor of the materials, as indicated in Eq. (3). The larger the  $\gamma_j$ -value is, the higher the dielectric loss (smaller  $Q$  factor). For the  $A_{2u}(\text{O}_{II})$  modes, the damping coefficient is smallest ( $(\gamma_j)_A = 29 \text{ cm}^{-1}$ ) for sample A, which possesses the largest  $Q \times f$ -value (248,000), and is the largest ( $(\gamma_j)_C = 36 \text{ cm}^{-1}$ ) for sample C, which possesses the smallest  $Q \times f$ -value (182,600). These results imply that the coherency of the vibrational mode is very sensitive to the ordering of the Ta- and Mg-cations. Substituting some Mg-ions for Ta-ions disturbs the uniformity of Ta–O bondings, which degrades the  $A_{2u}(\text{O}_{II})$  FTIR modes, since the  $\text{O}_{II}$ -layer is the layer sandwiched in between the two Ta-layers. Therefore, disorder leads to larger damping coefficient ( $\gamma_j$ ) of these modes, decreasing the quality factor ( $Q \times f$ -value) of the materials.

To facilitate the comparison, the difference in  $\gamma_j$ -value for B and C samples with respect to A samples was calculated,

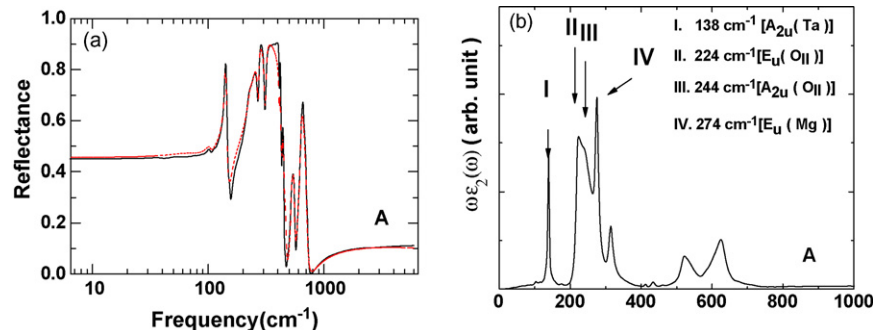


Fig. 3. Typical FTIR spectroscopy, (a) reflection spectra and (b) dielectric dispersion ( $\omega\varepsilon_2$ ) of the BMT materials.

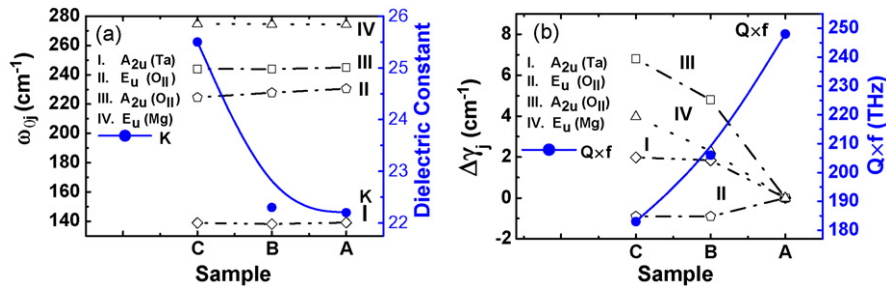


Fig. 4. Variation of (a) resonance frequency  $\omega_{0j}$ , (b) reduced damping coefficient ( $\Delta\gamma_j$ ), dielectric constant, and quality factor among the three BMT materials.

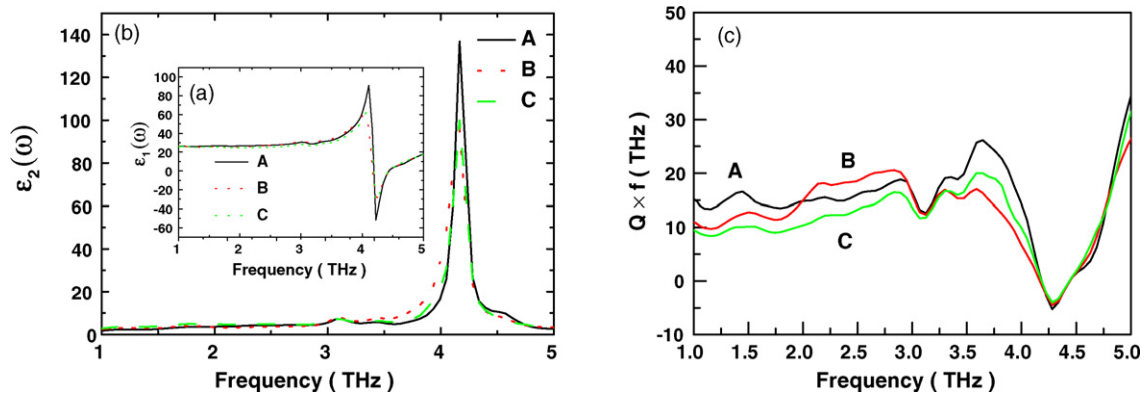


Fig. 5. Dispersion of (a) real part, (b) imaginary part of complex dielectric constant, and (c)  $Q \times f$ -values derived from FTIR spectra for three BMT materials.

resulting in reduced damping coefficient ( $\Delta\gamma_j$ ). Fig. 4(b) reveals that among the four major vibrational modes, the  $A_{2u}(O_{II})$  modes have most remarkable variation and the  $E_u(O_{II})$  modes have the least significant variation among the samples. Such a phenomenon is owing to the fact that the  $A_{2u}(O_{II})$  mode is the vibration of the  $O_{II}$ -layer out of plane towards the Ta-layer, whereas the  $E_u(O_{II})$  mode is the vibration of the  $O_{II}$ -layer in plane.

The FTIR spectra, the data processed using Kramers–Kronig relationship, explains very well the microwave dielectric properties of the BMT materials. The significance of such a phenomenon is that the same analyzing procedure can be used to estimate the dielectric properties of the materials in the terahertz regime. Fig. 5(a) and Fig. 5(b) show the real and imaginary parts of complex dielectric constant ( $\epsilon^* = \epsilon_1 + i\epsilon_2$ ) calculated in the FTIR frequency regime. Fig. 5(a) indicates that terahertz dielectric constant,  $K_{THz} \sim 26$ , varies insignificantly with the samples. Moreover, the dielectric constant derived from FTIR spectra,  $(K)_{FTIR}$ , is nearly the same as that measured at microwave frequency regime  $(K)_{6GHz}$ , indicating that there is no vibrational resonance mode in between microwave frequency and the terahertz regime (6 GHz–1 THz). This is an important factor for a high- $Q$  material, as the vibrational resonance modes occurred at low-frequency regime usually quite lossy and will degrade the  $Q$ -values for the materials.

The  $Q \times f$ -values calculated in 1–5 THz regime, where  $Q = \epsilon_1/\epsilon_2 = 1/\tan \delta$ , is shown in Fig. 5(c), indicating that the terahertz quality factor is also largest for sample A ( $(Q \times f_{THz})_A \sim 15$  THz at 1.0 THz regime), which possesses largest order-

ing parameters ( $S_A = 1.000$ ), and is smallest for sample C ( $((Q \times f_{THz})_C \sim 9.0$  THz at 1.0 THz regime), which possesses smallest ordering parameter ( $S_C = 0.966$ ). It should be noted that the rule of  $Q \times f = \text{constant}$  is true only when all the possible phonons have been included in the calculation, which is the case shown in Fig. 5. Restated, the dielectric properties at terahertz frequency regime estimated from FTIR spectroscopy vary with the samples in the same trend as the microwave dielectric properties at 6 GHz.

#### 4. Conclusion

The lattice vibrational modes of the BMT materials with different microwave dielectric properties were characterized by Raman and FTIR spectroscopies. These characteristics were correlated with the crystal structure parameters, including *cell volume* and *ordering parameter* of the materials. The decrease in the full-width-at-half-maximum (FWHM) of  $A_{1g}(O)$  Raman modes and the damping coefficient of the  $E_u(O_{II})$  and  $A_{2u}(O_{II})$  FTIR modes correlates very well with the increase in ordering parameter. Among the two spectroscopic techniques, the FTIR correlates with the dielectric properties of the BMT materials more directly. The dielectric constant of the materials at terahertz estimated from FTIR is around  $K_{THz} \sim 26$ , which is close to the  $K$ -value measured at microwave frequency regime ( $K_{6GHz} \sim 22$ –25). The FTIR spectroscopy can thus be used for estimating the dielectric properties of the materials in terahertz frequency regime.

## Acknowledgement

The authors would like to thank the National Science Council, Republic of China, for financially supporting this research under Contract Nos. NSC 94-2112-M-003-006 and NSC 95-2112-M-003-018-MY2.

## References

1. Surendran, K. P., Sebastian, M. T., Mohanan, P. and Jacob, M. V., The effect of dopants on the microwave dielectric properties of  $\text{Ba}(\text{Mg}_{0.33}\text{Ta}_{0.67})\text{O}_3$  ceramics. *J. Appl. Phys.*, 2005, **98**, 094114–094119.
2. Galasso, F. S., *Structure, Properties and Preparation of Perovskite-Type Compounds*. Pergamon, Oxford, 1969, pp. 13–15.
3. Tamura, H. D., Sagala, D. A. and Wakino, K., Lattice vibrations of  $\text{Ba}(\text{Zn}_{1/3}\text{Ta}_{2/3})\text{O}_3$  crystal with ordered perovskite structure. Part 1. *Jpn. J. Appl. Phys.*, 1986, **25**, 787–791.
4. Siny, I. G., Tao, R. W., Katiyar, R. S., Guo, R. A. and Bhalla, A. S., Raman spectroscopy of Mg–Ta order–disorder in  $\text{BaMg}_{1/3}\text{Ta}_{2/3}\text{O}_3$ . *J. Phys. Chem. Solids.*, 1998, **59**, 181–195.
5. Chia, C. T., Chen, Y. C., Cheng, H. F. and Lin, I. N., Correlation of microwave dielectric properties and normal vibration modes of  $x\text{Ba}(\text{Mg}_{1/3}\text{Ta}_{2/3})\text{O}_3-(1-x)\text{Ba}(\text{Mg}_{1/3}\text{Nb}_{2/3})\text{O}_3$  ceramics: I. Raman spectroscopy. *J. Appl. Phys.*, 2003, **94**, 3360–3364.
6. Chen, Y. C., Cheng, H. F., Liu, H. L., Chia, C. T. and Lin, I. N., Correlation of microwave dielectric properties and normal vibration modes of  $x\text{Ba}(\text{Mg}_{1/3}\text{Ta}_{2/3})\text{O}_3-(1-x)\text{Ba}(\text{Mg}_{1/3}\text{Nb}_{2/3})\text{O}_3$  ceramics: II. Infrared spectroscopy. *J. Appl. Phys.*, 2003, **94**, 3365–3370.
7. Spitzer, W. G., Miller, R. C., Kleinman, D. A. and Howarth, L. E., Far infrared dielectric dispersion in  $\text{BaTiO}_3$ ,  $\text{SrTiO}_3$ , and  $\text{TiO}_2$ . *Phys. Rev.*, 1962, **126**, 1710–1721.
8. Lin, I. N., Chia, C. T., Liu, H. L., Cheng, H. F. and Chi, C. C., Dielectric properties of  $x\text{Ba}(\text{Mg}_{1/3}\text{Ta}_{2/3})\text{O}_3-(1-x)\text{Ba}(\text{Mg}_{1/3}\text{Nb}_{2/3})\text{O}_3$  complex perovskite ceramics. Part 1. *Jpn. J. Appl. Phys.*, 2002, **41**, 6952–6956.